Proceedings of the ASME 2013 Fluids Engineering Division Summer Meeting
FEDSM2013
July 7-11, 2013, Incline Village, Nevada, USA

FEDSM2013-16598

NUMERICAL OPTIMAL DESIGN OF IMPELLER BACK PUMP-OUT VANES ON AXIAL THRUST IN CENTRIFUGAL PUMPS

Hong Feng
Research Center of Fluid Machinery Engineering and Technology, Jiangsu University
Zhenjiang, Jiangsu, China

Yuan Jianping
Research Center of Fluid Machinery Engineering and Technology, Jiangsu University
Zhenjiang, Jiangsu, China

Heng Yaguang
Research Center of Fluid Machinery Engineering and Technology, Jiangsu University
Zhenjiang, Jiangsu, China

Fu Yanxia
Research Center of Fluid Machinery Engineering and Technology, Jiangsu University
Zhenjiang, Jiangsu, China

Zhou Banglun
Research Center of Fluid Machinery Engineering and Technology, Jiangsu University
Zhenjiang, Jiangsu, China

Zong Weiwei
Research Center of Fluid Machinery Engineering and Technology, Jiangsu University
Zhenjiang, Jiangsu, China

ABSTRACT

Axial thrust in centrifugal pumps attracts extensive attention in order to improve the operating reliability of pumps. High axial thrust can cause rapid thrust bearing wear and subsequent pump failure or frequent overhauls. A centrifugal pump (XA65/20) was selected in this study, based on $L_{16}(4^3)$ orthogonal array and CFD methods. The time-averaged Navier-Stokes equation was calculated for a 3D steady flow in the model pump in ANSYS CFX with the standard k-ω turbulence model and standard wall function applied. The structured meshes with different numbers were used for comparison in order to confirm that the computational results were not influenced by the mesh. Meanwhile, the effects of impeller back pump-out vane geometrical parameters, including its thickness S_k, its outlet diameter D_e and axial clearance δ, on the axial thrust and performances of the model centrifugal pump were analyzed. The different orthogonal schemes were obtained on the different values of S_k, D_e, and δ.

Finally, when the parameters of the impeller S_k, D_e, and δ are 5mm, 100mm, 1.5mm, respectively. The Best Efficiency Point (BEF) of 69.9% was achieved with 60.12m for the designed head and -952.133N for the minimum total axial force. The corresponding impeller with minimum total axial force was considered as the optimal scheme and manufactured for experimental test. The external characteristics by CFD have a good agreement with their experimental data, which also better verified the accuracy of the numerical method of axial thrust applied in this research.

NOMENCLATURE

Q (m3/h)	Flow rate
S_k (mm)	Back pump-out vane thickness
δ (mm)	Axial clearance
D_e (mm)	Back pump-out vane outlet diameter
Z	Back pump-out vane number
N (r/min)	Rotating speed
ρ (kg/m3)	Density
g (m/s2)	Gravity acceleration
H (m)	Pressure head
ω (rad/s)	Angular speed
p (Pa)	Pressure

INTRODUCTION

One of the most challenging aspects in horizontal pumps design is represented by the accurate evaluation of the axial thrust acting on the rotating shaft. In order to balance axial thrust of centrifugal pumps, many devices such as balancing disk, balancing drum, balancing hole and sealing system are used [1]. However, many of these devices become complicated and cause problems such as the vibration by balancing disk [2]. Therefore, a very simple device to balance axial thrust is strongly demanded. Nowadays, back pump-out vanes applied to balance axial thrust have been widely used in the practical project for its simple structure, easy manufacture and lower cost than other devices such as balancing hole or balancing drum. However, structural design of back pump-out vanes were often just based on the engineering experience, irrational structures would not only decrease axial thrust but also could degrade the performances of centrifugal pumps. Therefore, how to optimize the design of back pump-out vanes to balance axial thrust and improve the performances of centrifugal pumps is a challenging problem.

In this paper, the model pump of XA65/20 was designed to study its axial thrust and external characteristics with S_k, δ and

D_e, chosen for its optimal design. An $L_{16}(4^3)$ orthogonal array was designed with the above three factors and four levels with SAS hybrid design method. Seven schemes were selected for axial thrust and external characteristics analysis. The axial thrust and performances were predicted by the commercial code ANSYS CFX. Five impellers with good external characteristics were chosen for further analysis. The distributions of pressure, turbulence kinetic energy and velocity were carefully analyzed. One impeller was chosen as optimal scheme and manufactured for experiments. The results confirm that it was feasible for the optimal design based on numerical simulation of orthogonal designed back pump-out vanes, the prediction by CFX was accurate and the whole work could offer reference to the optimum design of centrifugal pumps with the back pump-out vanes.

THEORETICAL ANALYSIS

Back pump-out vanes refer to several radial vanes mounted on the back shroud of impellers. The structure of prototype impeller is shown in Fig.1.

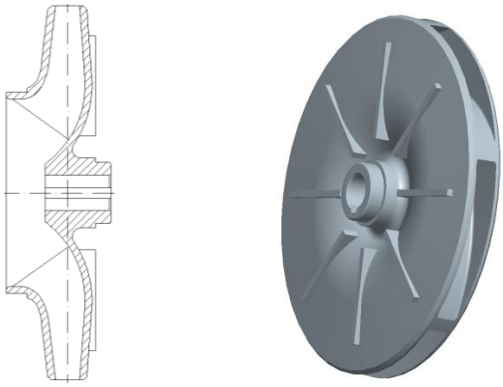

(1) LONGITUDINAL SECTION (2) SOLID MODEL

FIGURE.1 Impeller model

The pressure distribution of balancing axial thrust is shown in Fig .2. Without back pump-out vanes, it will generate axial thrust due to the asymmetric front and back shroud of the impeller, the size of the axial thrust is shown in the left shadow. If the impeller mounted with back pump-out vanes, the back pump-out vanes will rotate and drive the fluid in back pump chamber to rotate together. Then, part pressure head acted on the back shroud convert into velocity head, the pressure of the back pump chamber will decrease, shown in the right shadow. Therefore, the axial thrust acted on the impeller will decrease in consequence.[3]

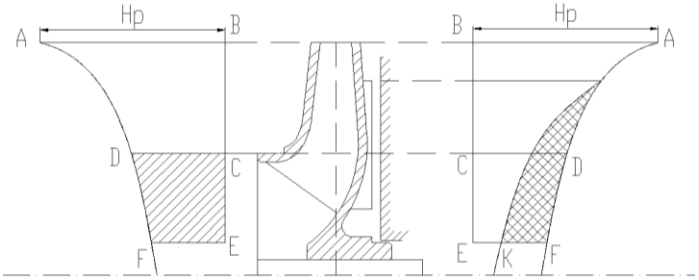

FIGURE.2 PRINCIPLE OF BALANCING AXIAL THRUST OF BACK PUMP-OUT VANES

For the axial thrust prediction of the model pump, the region concerning the axial thrust was divided into three parts, and the thrusts on each region were examined individually. One of them is the thrust that is acted on the front and back shroud. It is called F_{sh} in this paper. The other is the thrust that is acted on the pressure side and suction side of the impeller blades. It is called F_b in this paper. The last is the thrust generated by the surface of hub. It is called F_{sb} in this paper. Therefore, the total axial thrust acted on the impeller, it is called F_t in this paper, is the vector sum of F_{sh}, F_b and F_{sb} [4]. That is to say,

$$F_t = F_{sh} + F_b + F_{sb}$$

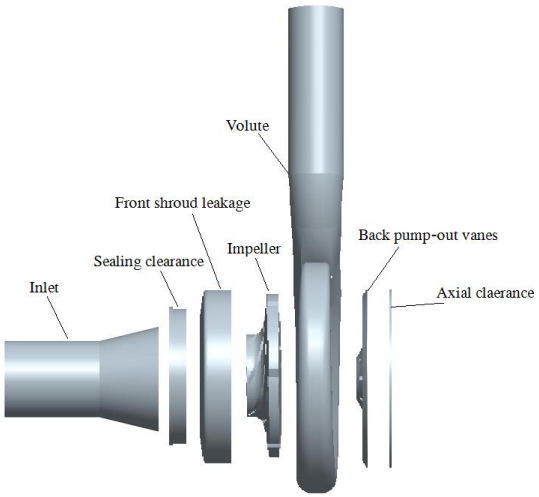

FIGURE.3 CACULATING DOMAINS

NUMERICAL SIMULATION

1 Calculating model

The calculating model was created based on the pump geometry and the whole flow domain consists of seven components: inlet section, sealing clearance, front shroud leakage, impeller passage, volute, back pump-out vanes passage and axial clearance, shown in Fig.3. After modeled in Pro/E, the assembly model is imported to ANSYS CFX 13 for calculating.

2 Mesh sensitivity analyses

The whole mesh generation was carried out by the ANSYS ICEM CFD 13 software, and the multi-block structured grid was utilized to discretize the computational domain. In spite of a very good general agreement between the numerically simulated and experimentally measured pressure values on the impeller, the axial thrust prediction was off by a significant amount [5]. In the theory, with the grid number increasing, the error caused by the grid will be reduced gradually until it disappears. However, considering the configuration and calculating time, the number of grid cannot be too large. In this paper, five different grid numbers were selected for the numerical simulation. To reduce the calculating deviation at the sealing clearance, 0.1×120 structured elements were generated in these special domains. The calculating models were covered with regular structure grids regularly, shown in Fig.4. This paper selected the grids size of 2.0 to improve calculating accuracy and shorten calculating time

TABLE.1 GRID SENSITITY ANALYSIS

Mesh Software	ANSYS ICEM CFD 13				
Global Size	1.6	1.8	2.0	2.2	2.4
Grids Number	3001254	2263152	1950807	1602135	1410235
H_R/m	52.9556	52.9554	52.9541	52.5102	52.5031
η_R/%	68.7845	68.7843	68.7826	68.2060	68.1968

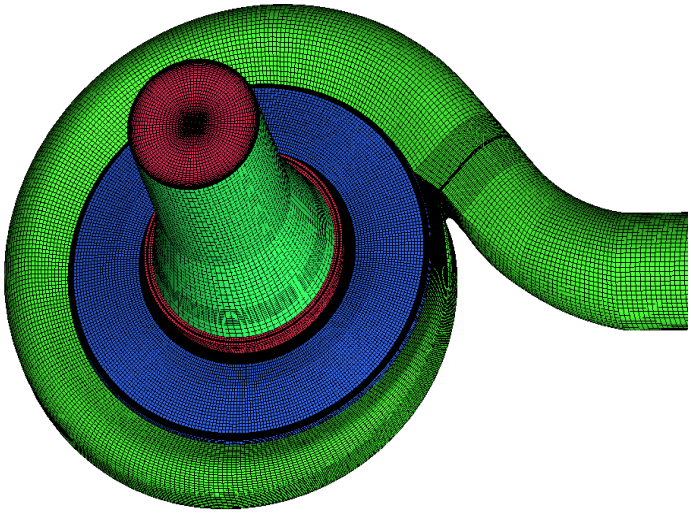

FIGURE.4 COMPUTATIONAL MESHES

3 Boundary conditions

The whole hydraulic passages of the model pump were taken as the computational domain. The flow domain was divided into 2 types of sub-domains and includes seven sub-domains, namely, inlet section, sealing clearance, front shroud leakage, blade passages, volute, back pump-out vanes passage and axial clearance. The inlet section, sealing clearance, front shroud leakage, volute and axial clearance belong to the first type sub-domain. The equations for this type region were solved in a stationary framework. The second type sub -domain is the impeller passage and the back pump-out vanes passage which are attached to the rotating frame and solved in a rotating framework via the Multiple Reference Frame (MRF), and the rotational speed was set as 2900 rpm. The interfaces are formed between the different regions [6].

A uniform axial velocity based on the mass-flow rate was specified at the inlet, and the outlet boundary is assumed to be opening. At the outlet pipes, there is an unavoidable effect on the final flow solution as a result of the boundary conditions. A reasonable length is added to the real machine geometry to avoid this effect as much as possible. This paper select the grids size of 2.0, and the value of y+ is 40, which indicates the near-wall nodes are not within the laminar sub-layer but within the log-low layer[7]. So the standard wall function is approached to the turbulent flow of near-wall, and all physical surfaces of the pump were set to be no-slip wall.

4 Turbulence model

In general terms the turbulence model describes the distributions of the Reynolds stresses in the flow domains. All turbulence models in use are of an empirical nature. So there is no universally valid turbulence model which will yield optimum results for all applications. In other words, it is important to select the most suitable turbulence model for the fluid domains to be calculated and to carefully validate it by comparing the numerical results with test data. Standard k-ω model, SST k-ω model, Standard k-ε model and RNG k-ε model are applied to carry out the numerical flow calculations. Tab.2 compares the test results and numerical data which are obtained with different turbulence models. The predicting results with Standard k-ω model are closer to the test data. Therefore, Standard k-ω model is the most model and chosen for the following numerical calculation.

TABLE.2 NUMERICAL RESULTS ON DIFFERENT TURBULENCE MODELS

Turbulence	Test	Standard	SST	Standard	RNG
Model	results	k-ω	k-ω	k-ε	k-ε
H_R/m	42.01	52.9541	53.2732	53.0497	53.6298
η_R/%	57.21	68.7826	69.1970	68.9067	69.6602

5 NUMERICAL ALGORITHMS

In this centrifugal pump numerical computation analysis, a commercially available CFD code, ANSYS CFX 13 has been used to study the complex three-dimensional turbulent flow through the pump at five operating points. CFX is a general purpose CFD code solving three dimensional Reynolds Averaged Navies-Stokes (RANS) equation for steady and turbulent fluid flow [8]. Many researchers have used this CFD code for numerical computation. Satisfactory and good agreements between the numerical and experimental results have been obtained. The flow model was complemented with Standard k-ω model and logarithmic-law functions for the near wall flow, consistent with the non-slip wall condition. Second order upwind discretization was used for the convective and the

diffusive terms. The time dependent term scheme was second order implicit [8]. The pressure-velocity coupling was calculated by means of the SIMPLEC algorithm, and the convergence precision on was set to be 10^{-5}. During the numerical study, the guidelines proposed in Ref. [9] were used and the numerical uncertainty was related to the change in certain reference values when different mesh refinements were considered. Thus, the values obtained were accurate and they can validate that the numerical results were correct.

BACK PUMP-OUT VANE OPTIMAL DESIGN

1 Design parameters

The main parameters of XA65/20 type pumps at five design conditions are shown in Tab. 3

2 Back pump-out vane optimal design

Three factors including thickness S_k, outlet diameter D_e, and axial clearance δ were selected for optimal design. An L_{16} (4^3) orthogonal experiment was designed with the above three factors and four levels. Since the performances of prototype pumps cause large axial thrust and cannot satisfy the required pressure and efficiencies. After a serious of numerical simulations, seven impellers were chosen for further analysis. Their geometry parameters are shown in Tab.4. The simulating results of external characteristics are shown in Fig.5.

TABLE 3 MAINDESIGN PARAMETERS AT FIVE DESIGN CONDITIONS

Working conditions	Flow rate	Pressure head	Efficiency	Power	Rotating speed
	(m^3*h^{-1})	(m)	(%)	(kw)	($r*min^{-1}$)
$0.6Q_R$	66	66	63	≦30	2900
$0.8Q_R$	88	61	70		
$1.0Q_R$	110	57	74		
$1.2Q_R$	132	52	74.5		
$1.4Q_R$	154	46.5	71.5		

TABLE 4 PARAMETERS OF EITHT DESIGN SCHEMES AND PROTOTYPE

	S_k	δ	D_e	Z
Prototype	4	3	90	8
Scheme 1	2	2	100	
Scheme 2	5	1.5	80	
Scheme 3	6	1.5	85	
Scheme 4	6	2	100	
Scheme 5	2	4	85	
Scheme 6	5	4	80	
Scheme 7	5	1.5	100	

The simulation results were compared with the simulating results of prototype pump, as shown in Fig.5. The outlet diameter of scheme 1, scheme 4 and scheme 6 are the same and greatest among all the schemes, including the prototype pump. The pressure heads of scheme 1 are greater than other schemes at five working conditions. The pressure heads of scheme 4 are greater than scheme 6 around the designed flow rate, which are contrary to the phenomena at low and high flow rate. The pressure heads of scheme 2 are smaller than that of scheme 6, indicating that outlet diameter plays an important role on the pressure head of centrifugal pumps with pump-out vanes. Since the axial clearance of scheme 2 is smaller than scheme 7, the angular speed of the fluid in axial clearance of scheme 2 are greater than that of scheme 7, causing less leakage losses, the pressure heads of scheme 2 are greater.

The efficiency of scheme 1, scheme 4 and scheme 6 are also greater than other schemes. The efficiency comparisons of scheme 2, scheme 6 and scheme 7 shows that the efficiency can be increased by increasing the outlet diameter and increasing the axial clearance. Since the efficiency of scheme 1 is greater than that of scheme 4 at $0.6Q_R$, $1.0\ Q_R$, $1.2Q_R$, but opposite at $0.8Q_R$, $1.4Q_R$, there is no direct linear relationship between the efficiency and the thickness.

The total axial thrust of scheme 7 is smaller than other schemes, indicating that scheme 7 is optimal scheme among the whole orthogonal schemes in the point of reducing axial thrust. The total axial thrust comparison of scheme 2, scheme 7, scheme 1 and scheme 4 show that the total axial acted on the impeller can be reduced by reducing the axial clearance and increasing the outlet diameter. Total axial thrust decreased with the increase of flow rate. Namely, the effect of back pump-out vanes to balance axial thrust become more and more stronger at larger flow-rates working conditions

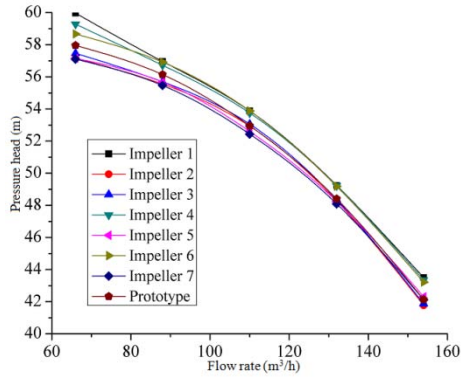

(1) FLOW-HEAD CURVES

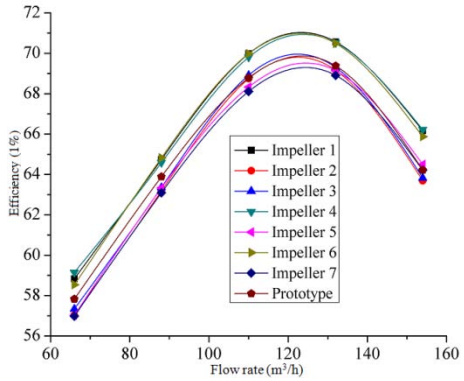

(2) FLOW-EFFICIENCY CURVES

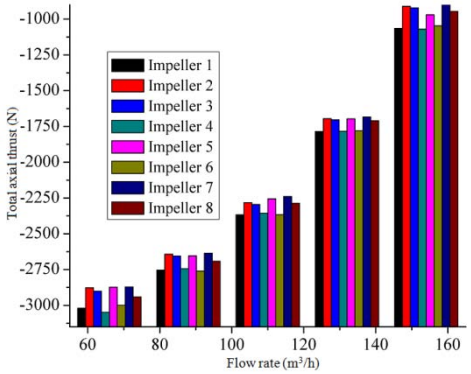

(3) TOTAL AXIAL THRUST

FIGURE.5 Numerical performance comparisons

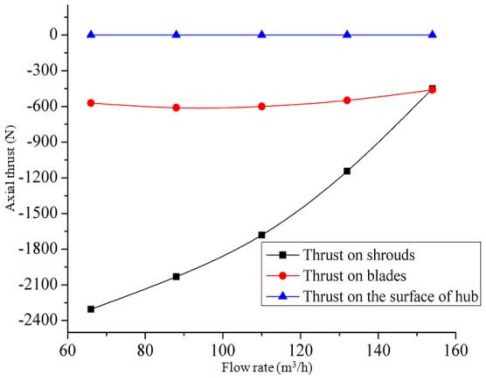

FIGURE.6 BREAKDOWN OF TOTAL AXIAL THRUST OF IMPELLER 7

The total axial thrust of impeller 7 were decomposed into several elements of thrust and analyzed in detail, shown in Fig.6. The axial thrust acted on the surface of the hub (F_{sb}) is very few, which is nearly to zero, so that the total thrust (T_t) is almost made up by the thrust on the shrouds (F_{sh}) and the thrust acted on the blades (F_{sb}) of the impeller, it is the same law with total axial thrust of other schemes. With the increase of flow rate, the total axial thrust acted on the front and back decreased sharply, while it is very slowly of the total axial acted on the blades in impeller 7.

3 Comparisons of internal flow field at designed discharge

The scheme 1, scheme 2, scheme 4, scheme 6 and scheme 7 are selected for further analysis. The impellers of scheme 1, scheme 4, and scheme 6 have better external characteristics, and the F_t of scheme 7 is the lowest.

Fig.7 shows the velocity contour of above five schemes at designed discharge. There is no significant difference in the impeller or volute passage between these five schemes. The contour comparison of scheme 2 and scheme 7 shows that the velocity distributions vary with different thickness clearance, so that it cause lower axial thrust in impeller 7.

Axial thrust acted on the pressure surface of blades in each impeller is shown in Tab 5.The thrust of impeller 7 is the lowest, and it is less 86.14N than scheme 6. The reason is that the pressure acted on the surface of blades in scheme 7 is smaller than that in impeller 6.

Velocity distributions on middle suction of axial clearance are given in Fig.9. The distributions are more regular in scheme 2 and scheme 6.The velocity and distribution ranges near the casing tongue in scheme 1, scheme 4 and scheme 7 are larger, as a result of lager outlet diameter of the back pump-out vanes in the three impellers.

The streamline distributions on the middle suction of back pump-out vanes are given in Fig.10. Several obvious vortexes are predicted in the middle section of all the five schemes, which inevitably lower the pump efficiencies. Relatively, there is less vortexes in the middle back pump-out vanes passage of scheme 6, so the efficiency of impeller 6 is the greatest at the designed flow rate, shown in Fig.5.

Turbulent kinetic energy is used to describe the turbulent pulsation level. Its value and spatial non-uniformity show the level and range of pulsing diffusion and viscous dissipation to a certain extent. The turbulent kinetic energy distributions of above five schemes are given in Fig.11. As predicted, near the casing tongue, the turbulent kinetic energy in scheme 1, scheme 4 and scheme 7 distribute in a large range with greater values relatively, which indicate the drastic movement of flow. The turbulent kinetic energy in scheme 6 distribute in limited ranges with lower values. Comparison of Fig.10 and Fig.11 show that all the predictions of turbulent kinetic energy are in good accordance with the predictions of streamline distributions.

TABLE 5 THRUST ON THE PRESSURE SURFACE OF BLADES

	Scheme 1	Scheme 2	Scheme 4	Scheme 6	Scheme 7
Axial thrust /N	1192.78	1137.74	1186.64	1193.01	1106.87

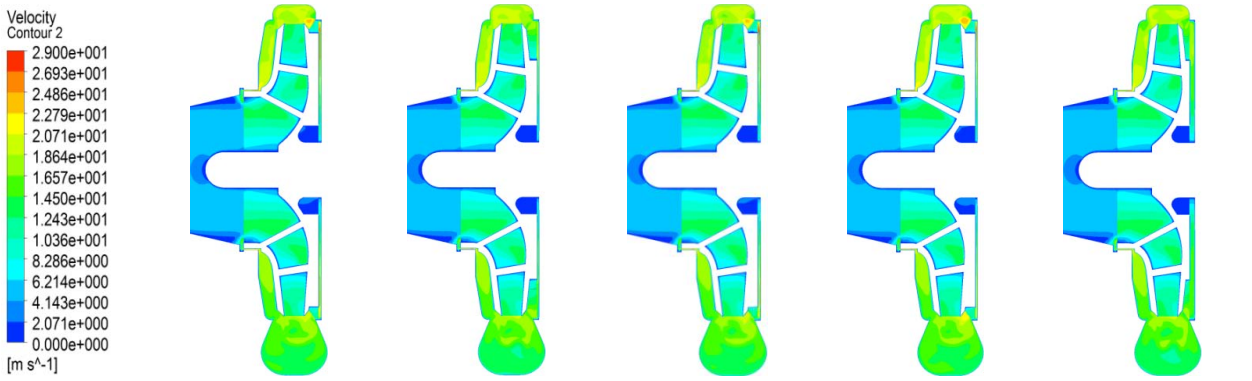

(1) IMPELLER 1 (2) IMPELLER 2 (3) IMPELLER 4 (4) IMPELLER 6 (5) IMPELLER 7

FIGURE.7 Velocity distributions in impellers

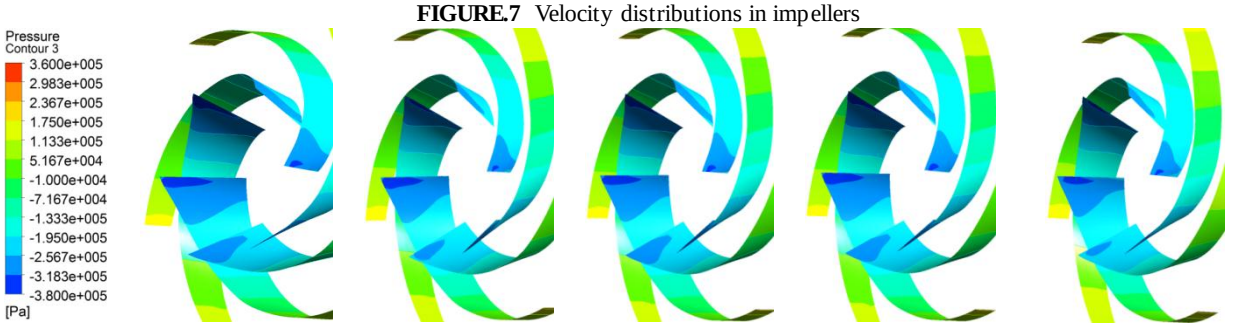

(1) IMPELLER 1 (2) IMPELLER 2 (3) IMPELLER 4 (4) IMPELLER 6 (5) IMPELLER 7

FIGURE.8 Pressure distributions on blades

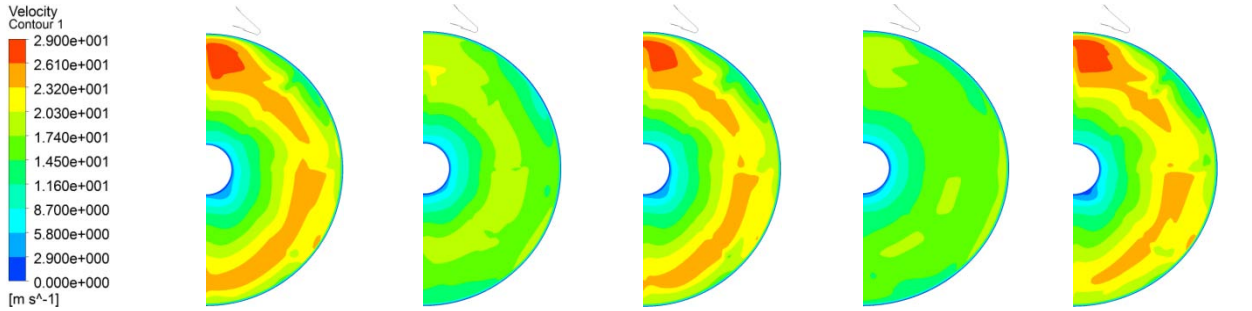

(1) IMPELLER 1 (2) IMPELLER 2 (3) IMPELLER 4 (4) IMPELLER 6 (5) IMPELLER 7

FIGURE.9 Velocity distributions on middle suction of axial clearance

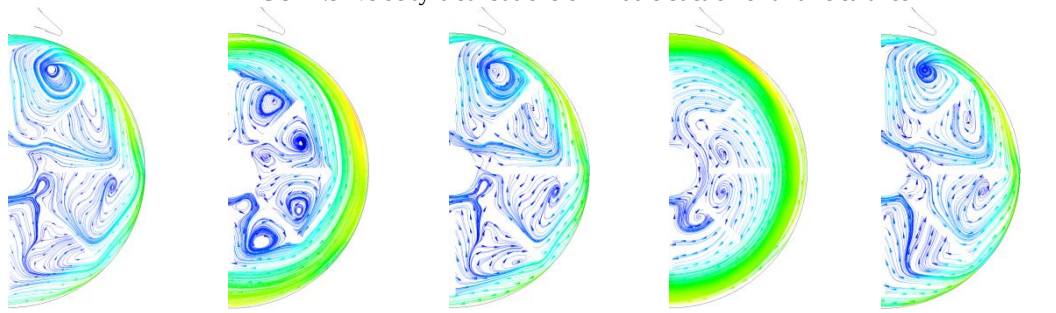

(1) IMPELLER 1 (2) IMPELLER 2 (3) IMPELLER 4 (4) IMPELLER 6 (5) IMPELLER 7

FIGURE.10 Streamline distributions on middle suction of back pump-out vanes

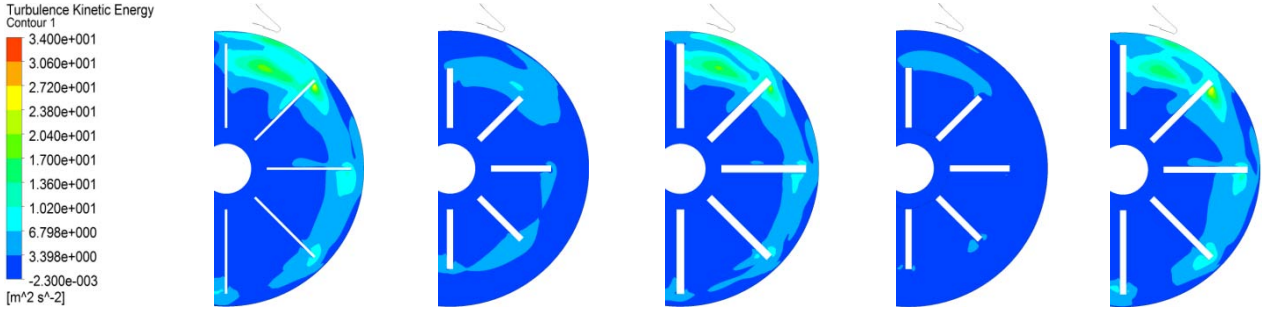

(1) IMPELLER 1 (2) IMPELLER 2 (3) IMPELLER 4 (4) IMPELLER 6 (5) IMPELLER 7

FIGURE.11 Turbulence kinetic energy distributions on middle suction of back pump-out vanes

EXPERIMENTAL CONTRAST

1 Test facilities

In order to analyze the accuracy of the simulation results, the XA65/20 pump fitted with impeller 7 and prototype impeller are both manufactured and tested. As shown in Fig.12, the experiment was conducted in Fujian Yinjia Electromechanical Co., Ltd. The pressure both in the inlet and outlet was measured by two pressure transmitters. The volumetric flow rate of the test was measured by a turbine flowmeter. The torque and shaft rotating speed were measured by a torque meter with the experimental data sending to the microcomputer of the pump comprehensive test system.

2 Test results

Figure 13 shows the comparisons of the pump performance curves between simulation and experiment. For the optimal impeller, the deviation of pressure heads and efficiency between test data and simulating results at the five operating conditions do not exceed 10% and 10.9%, while 11.7% and 12% for the prototype impeller, relatively. So it means that the hydrodynamic flow phenomenon in the pump was successfully reproduced in CFX, and therefore the prediction of axial thrust in this paper has a certain degree of accuracy.

FIGURE.12 TEST RIG AND TEST SYSTEM

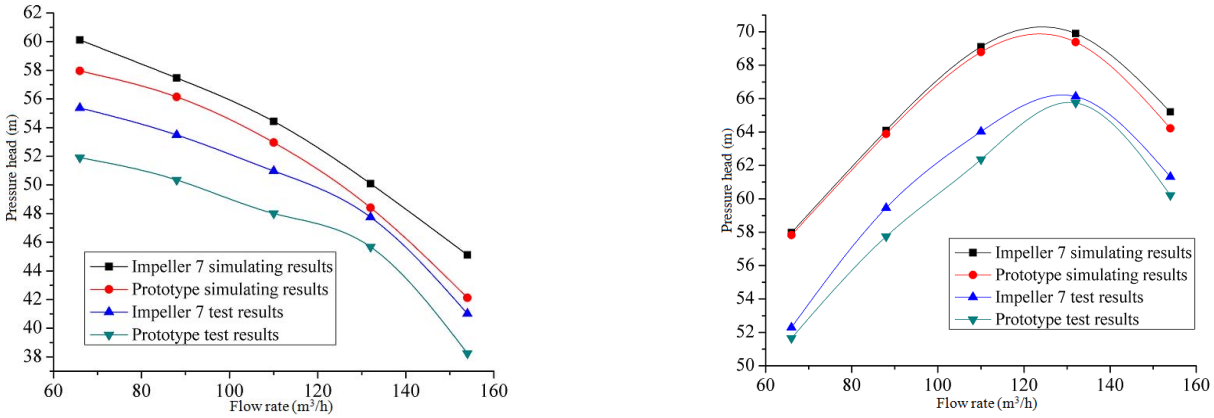

(1) FLOW- HEAD CURVES (2) FLOW-EFFICIENCY CURVES

FIGURE.13 Test performance comparisons of optimal scheme and prototype impeller

CONCLUSIONS

Based on L16 (43) orthogonal array and CFD methods, the prediction of axial thrust and external characteristics were carried out for model pump of XA65/20. It is summarized as follows.

1. It was shown that the axial thrust forces acted on the centrifugal pumps can be predicted by using CFD technology with practical accuracy, and numerical methods has been verified to achieve the optimal scheme selection from an orthogonal table by comparing the calculating results with the corresponding experimental data.

2. It was found that the total axial thrust varies according to the various flow rate, and it is almost made up by the thrust on the shrouds and the thrust acted on the blades of impeller.

3. The performances of XA65/20 pumps at five operating points are improved. The pressure head is increased by 3.46m at maximum. The pump efficiency is improved by 1.71% at 1.0 Q_R. The axial thrust is deduced by 100.3N at maximum.

ACKNOWLEDGEMENTS

This study is supported by National Natural Science Foundation of China, "Mechanism of vibration and nose induced by unsteady flow in a centrifugal pump" (Grant NO. 50979034.)

REFERENCE

[1] Ichiro Harada, Katsutoshi Kobayasi and Shigeyoshi Ono. Prediction of Axial Thrust for Mixed-Flow Pumps with Vaned Diffuser by Using CFD[J]. International Journal of Fluid Machinery and Systems, 20103(2):160-168.

[2]Heishiro ABE, Kazunari MATSUMOTO, Junichi KUROKAWA, et al. Analysis and Control of Axial Thrust in Centrifugal Pump by Use of J-Groove[J]. 23rd IAHR Symposium-Yokohama, 2006.

[3] GUAN Xingfan. Modern pumps theory and designe[M]. Beijing: China Astronautics Press, 2011

[4] Stepanoff A J. Centrifugal and axial flow pumps[M]. 2nd Cd. New York: John Wiley & Sons. Inc, 1957.

[5] K. N. Oliphant and D. Japikse. Experimental and numerical results of the coupled seal cavity and main flow for a liquid hydrogen rocket turbopump[J]. In 35th AIAA/ASME/SAE/ASEE Joint Propulsion Conference and Exhibit, June 1999. AIAA Paper 99-2825

[6] Gulich JF. Centrifugalpumps.Berlin Heidelberg, New York: Springer, 2007

[7] Wang FJ, Li YJ, Cong GH, et al. CFD simulation of 3D flow in large-bore axial-flow pump with half-elbow suction sump[J], J Hydro, Ser. B 2006; 18: 234-247

[8] Gonzalez J, Parrondo J, Stantolaria C, Blanco E. Steady and unsteady radial forces for a centrifugal pump with impeller to tongue gap variation[J]. J Fluid Eng 2006; 128: 454-462.

[9] Freitas, C.J. Journal of Fluids Engineering Editorial Policy Statement on the Control of Numerical Accuracy[J]. J Fluid Eng 1993;115:339-340.

[10] J.Kurokawa, T.Toyokura. Study on Axial Thrust of Radial Flow Turbomachinery[J]. 2nd International JSME Symposium Fluid Machinery and Fluidics, 1972; 204:31-40.